ACS APPLIED NANO MATERIALS

Article

Graphene Oxide-Coated CuO Nanoparticles for Functionalization of Acetylsalicylic Acid and Diclofenac

Anastasia Tkach, Anna Matsukovich, Nina Krekoten, Ljudmila Tabulina, Vladimir Labunov, and Darya Radziuk

ACS Appl. Nano Mater., **Just Accepted Manuscript** • DOI: 10.1021/acsanm.0c00852 • Publication Date (Web): 18 May 2020

Graphene Oxide-Coated CuO Nanoparticles for Functionalization of Acetylsalicylic Acid and Diclofenac

*Anastasia Tkach,[1] Anna Matsukovich,[2] Nina Krekoten,[3] Ljudmila Tabulina,[1] Vladimir Labunov[1] and Darya Radziuk[1]**

[1]Laboratory of Integrated Micro- and Nanosystems, Belarusian State University of Informatics and Radioelectronics, P. Brovki Str. 6, 220013 Minsk, Republic of Belarus

[2]B.I. Stepanov Institute of Physics, National Academy of Sciences, Nezavisimosti Ave. 68, 220072 Minsk, Republic of Belarus

[3]Scientific-Technical Center "Belmicrosystems", Kazintsa Str. 121 A, 220108 Minsk, Republic of Belarus

KEYWORDS: graphene, NSAID, copper oxide, ultrasound, nanocomposite.

ABSTRACT A single step ultrasonic method (20 kHz, 18 W/cm^2) is demonstrated for the functionalization of pristine nonsteroidal anti-inflammatory drugs: acetylsalicylic acid and diclofenac with preformed graphene oxide-coated CuO nanoparticles. These nanoparticles are positively charged and have a flower-like morphology with a mean size < 340 nm consisting of a pure CuO phase. Ultrasound causes complexation of each drug with these nanoparticles and, as a consequence, new advanced pharmaceutical nanocomposites: acetylsalicylic acid-graphene oxide-coated CuO and diclofenac-graphene oxide-coated CuO are formed. The surface composition and electronic molecular structure of these nanocomposites is modified at pH from 1 to 8 through the specific interactions involving Cu-O, C-H and H-bond formation with the carboxylic and carbonyl groups of acetylsalicylic acid, diclofenac and graphene oxide.

1. Introduction

Acetylsalicylic acid (ASA) and diclofenac are nonsteroidal anti-inflammatory drugs (NSAIDs) that are commonly prescribed to treat the inflammatory disorders and also cancer.[1-3] Salicylic acid (SA) is a product of ASA hydrolysis with valuable anti-inflammatory activity and analgesic potency.[4,5] The absorption rate and extent of ASA and salicylate in the gastrointestinal lumen can be modulated by their pH-dependent molecular electronic structure. The gastric metabolism of ASA, in which the acetyl moiety binds covalently to proteins and other molecules in the stomach wall, is consistent with its gastric toxicity, and its analgesic activity increases with the raised availability of the intact drug.[6] Only recently the effects of ASA on the platelet functions are better understood so that new methods can be developed to lessen in extent of harmful gastrointestinal damage.[7]

In contrast to ASA, diclofenac inhibits cyclooxygenase COX-2 enzyme with greater potency, retains antidepressant and anxiolytic response in patients with pain, but leads to serious cardiovascular and renal side effects.[8] Similarly to ASA, diclofenac also causes severe dose-dependent gastrointestinal injury.[9] The pharmaceutical effects of diclofenac are frequently associated with the formation of H-bonds between its carboxyl group and several side chains of the COX enzymes.[10] The modulation of the n-π^* interaction and its interrelation with the H-bonding can help to benefit from the biological activity of diclofenac.[11] Up to now this knowledge has been applied for the transformation of pristine diclofenac compound into various modes of liquid-filled soft gel capsules[12] or submicron particles in a tablet to treat osteoarthritis, rheumatoid arthritis, and cancer-related pain.[13,14] In consequence, modified diclofenac caused fewer digestive and central nervous system-associated side effects than ASA.[15] However, still both ASA and diclofenac in their most frequent form, i.e. oral tablet, unavoidably lead to a

bleeding of the gastrointestinal system and this damage is dose dependent.[9] Therefore, there is a need to find new healthier approaches to reduce the dosage of these NSAIDs and enhance their therapeutic efficiency.

It has been shown that the anti-inflammatory activity of many NSAIDs can be significantly improved through their metal complexes.[16] Metal complexes and metallodrugs are in the existent clinical use to treat inflammation ailment, diabetes, bacterial infections and many types of cancer.[17-21] Among them copper (II) complexes with NSAIDs exhibit excellent ability to cleave the pathogenic DNA and participate in the formation of H-bonds at the DNA surface.[22] Nowadays both *in vitro* and *in vivo* studies confirm the enhanced anticancer and anti-inflammatory effects of Cu(II)-NSAIDs complexes.[23] For example, the copper-ASA complexes exhibit more potent anti-inflammatory and anti-thrombotic activity than free drug resulting in a fewer side effects in rats or mice.[24,25] Such advanced pharmacological activity of this compound is related to its final crystal structure, the specific coordination to water molecules via H-bonding and the improved COX-1/COX-2 selectivity. The compounds based on the Cu(II) complexation with diclofenac exhibit good antitumor and antimicrobial activity.[18,25] For example, tetranuclear copper(II) complexes containing multiple diclofenac and Schiff base moieties exhibit cytotoxic effect on cancer stem and bulk breast cancer cells by elevating intracellular reactive oxygen species (ROS) levels and inhibiting COX-2 expression.[26] In another study, copper(II)-phenanthroline complexes bearing diclofenac demonstrate preferential potency towards bulk breast cancer cells over breast CSCs.[27]

In many compounds ASA or diclofenac are bonded to the central Cu atom through the carboxyl groups and some of them had been constituting an important element of commercially available anti-inflammatory drugs since 2001.[28,29] However, most of the existing Cu(II)-NSAID

complexes have weakly bound carboxylic acid ligands and can easily dissociate favoring the interaction of $O_2\cdot$ radicals with the free sites of copper. Therefore, it is necessary to understand the electronic molecular surface structure of Cu(II)-NSAID complexes in aqueous solution at different pH values in order to improve their functions.

The solubility, bioavailability, absorption and cell penetration of NSAID to the site of action are strongly correlated with the H-bond formation and depend on the ionization form of the pharmaceutical compound.[30] Nonionized species of the drug compound are major forms in the stomach and in the upper small intestine.[31] Drug molecular compounds undergo ionization to different extents in various parts of the body and this process is pH-dependent.[32] About 85% of marketed drugs contain functional groups that are ionized to some extent at physiological pH (1.5-8). However, if the compound forms many hydrogen or ionic bonds with water, the desolvation becomes compelling. Therefore, an oral drug should follow the Lipinski "rule of five" to be able to remain unimpaired at acidic conditions within the stomach (pH=1-3), undergo absorption through the intestine and be soluble in a blood before it reaches the required area.[33]

In nanomedicine, nanoscale carriers can significantly enhance the bioavailability of drug and decrease the dose of administration by utilizing safer methods for modification of NSAIDs with metals and carbon-based substances.[34,35] Among nanoscale carriers graphene oxide (GO) is biocompatible,[36] bactericidal[37] and can provide high surface area enriched with carboxyl, carbonyl, hydroxyl and lactone groups useful for the complexation with copper.[38] The operation of CuO nanoparticles lie beyond their antibacterial effects[39] because of specific optical[40] electrical,[41] and magnetic[42] morphology-dependent properties that can be beneficial for pharmaceutical purposes. The mergence of CuO and GO into a new nanocomposite significantly

improves antibacterial activity,[43] enhanced anticancer catalytic sensing[44] and specific binding ability of drugs.[45]

In aqueous solution ultrasound produces acoustic cavitation and so sonochemistry.[46,47] The synergetic effects of sonochemical reactions and high energy gradients in hot spots have been successfully applied for the synthesis of various nanomaterials with enhanced antibacterial functions.[48,49] One can find much information about the CuO nanoparticle formation and its interaction with carbon dots and textile material or polymers by using the fundamental principles and mechanisms of sonochemistry. At present, this knowledge is restricted to CuO-GO formation, and the interaction of this new nanomaterial with ASA or diclofenac is not revealed.

For this reason, the aim of our work is to develop a new single step method in the use of ultrasound (20 kHz) for the graphene oxide-coated CuO nanoparticle formation and subsequent functionalization of this material with pristine NSAIDs: ASA or diclofenac. The goal is to disclose the specific binding of ASA and diclofenac to graphene oxide-coated CuO nanoparticles as a result of complexation produced by ultrasound. To do so, we proposed to study the changes of the electronic molecular structure of final products: ASA-GO-CuO and diclofenac-GO-CuO nanocomposites in aqueous solution being adjusted to pH = 1, 5 or 8 that is closer to the intraluminal media of stomach,[50] human gastrointestinal tract,[51] and duodenum.[52] The complexation of ASA or diclofenac with CuO and GO can be of use in the understanding of the NSAID-metal and NSAID-graphene interaction, activation of NSAIDs by metal ions and oxides. New knowledge can be applied to fundamental intracellular studies of the NSAID-enzyme (COX, LOX, etc.) reactions that are of great significance in *in vivo* studies.

2. Experimental Section

Materials and Synthesis. Graphite (9-47 μm dispersion) with elemental composition: C (95.0 ± 2.0 atom.%), O (4.0 ± 1.0 atom.%), Ti (0.1 ± 0.0 atom.%), Ca (1.1 ± 0.1 atom.%). $Cu(CH_3COO)_2$ H_2O, H_3PO_4, $KMnO_4$, H_2SO_4, H_2O_2 (60 %), HCl (35 %), HNO_3 (40 %), C_2H_5OH, C_3H_8O, KOH (44 %), NaOH and NH_4OH are obtained from Belreachim JSC (Republic of Belarus). Deionized water (pH = 5.5, specific conductivity 5 $\mu S \cdot cm^{-1}$) was prepared by using a homemade distillation apparatus (Republic of Belarus). We synthesized graphene oxide (GO) using the improved Hummers method[53] and applied centrifugation (4.293 g) for multiple rinsing, at first, with deionized water (pH = 5.5) for a total duration of 450 min and, at second, with a mixture of {deionized water : isopropanol} at a volume ratio 1:3 for a total duration of 90 min (more details in supporting information). The final GO product was obtained after drying at 100°C in the air.[54] Pristine NSAIDs: ASA and diclofenac sodium were purchased from Bayer AG (Germany) and Holden Medical B.V. (The Netherlands). For experiments 10 tablets of each NSAID were grinded to fine powder. The aqueous solution of ASA or diclofenac were prepared by dissolving a powder of this drug in deionized water (pH = 5.5) under continuous stirring at a critical concentration of dissolution at room temperature according to literature.[55,56] For experiments both NSAID aqueous solutions were filtered through a cellulose membrane filter (red line, the pore size 8-12 nm).

a) Sonochemical formation of graphene oxide-coated CuO nanoparticles

At first, copper oxide nucleation centers were formed via the co-precipitation chemical reaction in a solution containing 50 mL of liquid NH_4OH, 1.82 g of 0.2 M $Cu(CH_3COO)_2$ H_2O and 0.80 g of 0.4 M NaOH. This solution was heated under vigorous stirring until the temperature has reached 80°C. Since that moment 7 mL of deionized water (pH = 5.5) was

dropwise added into this heated solution under continuous stirring every 10 min during the total duration of 150 min followed by the formation of dark brown sediment on the bottom of the vessel. Then the obtained colloidal solution was cooled down to room temperature, triply rinsed with deionized water and once with isopropanol by using centrifugation (8.117 g). At second, the aqueous solution of GO, which has been previously sonicated in solution containing 10 mL of deionized water and 10 mL of isopropanol, was added to this sediment (6.8 mg). Sonication (20 kHz, 18 $W \cdot cm^{-2}$) of this aqueous solution with GO was assisted with the mechanical stirring for 30 min in the open air. Then the final product was triply rinsed with deionized water and once with isopropanol by using centrifugation (8.117 g) for 20 min, then dried at 100°C.

The control experiment was performed by applying ultrasound (20 kHz, 18 $W \cdot cm^{-2}$) to the colloidal mixture of GO and preformed copper oxide powder (synthesized without GO and dried at 400°C in the air) during 15 min under continuous stirring. Then this colloidal solution was stored for 12 h at room temperature. Finally the product was triply rinsed with deionized water and once with isopropanol by using centrifugation (8.117 g) for 20 min and dried at 100°C.

In all our sonochemical experiments we used a homemade horn-type ultrasonic disperser N.4-20 operating in a continuous mode at 20 kHz frequency designed by Cavitation Inc. (Belarusian State University of Informatics and Radioelectronics, Republic of Belarus, **Figure S1** in supporting information). We applied a method of calorimetry[54,57] to calibrate this device (**Figure S2**, more details in supporting information).

The synthesis of nanocomposites was also conducted at different molar and volume concentration of precursor compounds in order to investigate the GO-CuO morphology evolution. At first, 25 mL of aqueous solution of 125 mM $Cu(CH_3COO)_2$ H_2O and 25 mL of 500 mM NaOH were dissolved in 15 mL of liquid NH_4OH and heated under vigorous stirring to

T = 80°C. During heating this solution was dropwise added by 65 mL of deionized water (pH = 5.5) until we observed the appearance of dark green-brown sediment on the bottom of the vessel. Afterwards the solution was cooled down to the room temperature and the sediment was triply rinsed with deionized water (pH = 5.5) and once with isopropanol by centrifugation (8.117 g). In the next place, 2.5 mg of preformed GO was added to the sediment and sonicated under vigorous stirring for 30 min at 18 $W \cdot cm^{-2}$. In another procedure, 25 mL of aqueous solution of 0.2 M $Cu(CH_3COO)_2$ H_2O and 25 mL of 0.2 M NaOH were dissolved in 50 mL of liquid NH_4OH and heated under vigorous stirring until T = 80°C. Then this solution was dropwise added by 6.8 mg of GO and 100 mL of deionized water during 190 min of continuous stirring with sonication (at 18 $W \cdot cm^{-2}$). The sediment was formed by centrifugation (8.117 g) and triply rinsed with deionized water and once with isopropanol followed by drying at 100°C.

b) Ultrasonic functionalization of pristine acetylsalicylic acid or diclofenac with graphene oxide-coated CuO nanoparticles

30 mg of sonochemically formed graphene oxide-coated CuO nanoparticles was added by 30 mg of ASA or diclofenac in 11 mL of deionized water (pH = 5.5) and treated by ultrasound for 3 min (20 kHz, 18 $W \cdot cm^{-2}$) under air in a vessel placed in the ice bath. After that the colloidal suspension was triply rinsed with deionized water by centrifugation (8.117 g) for a total duration of 45 min and dried at 100°C in air to obtain a powder. Several control experiments were accomplished by ultrasound (3 min, 20 kHz, 18 $W \cdot cm^{-2}$): 1) the mixture (60 mg) of GO and free NSAID at a mass ratio 1:1, and 2) the mixture (60 mg) of preformed CuO nanoparticles and free NSAID at a mass ratio 1:1; 3) aqueous solution of pristine ASA or diclofenac (30 mg in 11 mL of deionized water) of 1, 3, 5, 10 and 15 min length in order to find out the effect of ultrasound

on the chemical structure of each drug. After experiments solutions were triply rinsed with deionized water by centrifugation (8.117 g) and dried at 100°C in the open air.

c) pH test of acetylsalicylic acid-GO-CuO and diclofenac-GO-CuO nanocomposites

30 mg of acetylsalicylic acid-GO-CuO or diclofenac-GO-CuO nanocomposites were added by 3 mL of aqueous solution at pH=1, 5 or 8 and stored at room temperature. The aqueous solution at pH = 1 was obtained by the addition of 1N HCl and at pH = 8 – by the addition of 44 % of KOH aqueous solution. Samples were withdrawn after 7 h, triply rinsed by centrifugation (8.117 g) for 15 min in order to remove the unreacted chemical residuals. The obtained sediment was dispersed by deionized water (3.5 mL) and studied by UV-Vis absorption spectroscopy by using quartz cuvette SUPRASIL Hellma Analytics 111-QS (Z600725) with a pathlength of 10 mm. The presence of NSAIDs was examined by their characteristic UV-Vis absorption peaks at 276 nm (ASA), ~ 300 nm (salicylic acid) and 277-280 nm (diclofenac).

Equipment and Analytical Methods. Synthesized nanoparticles and nanocomposites were characterized by scanning electron microscopy (SEM) and energy dispersive X-ray fluorescence spectroscopy (EDS), X-ray powder diffraction (XRD), dynamic light scattering (DLS), zeta potential (ZP), Raman microscopy, Fourier transform infrared (FTIR) and UV-Vis absorption spectroscopy methods. Their morphology and elemental composition were defined by SEM (S-4800) Hitachi, Japan. The phase composition was identified by using the powder diffraction patterns recorded with an EMPYREAN diffractometer (PANalytical, The Netherlands) using Cu-Kα radiation (Ni-filter) at 296 K. The crystallite thickness *S* (of GO-CuO nanoparticles) was determined by the Scherrer's equation (1):

$$S = \frac{K \cdot \lambda}{B \cdot \cos\theta_B}, \qquad (1)$$

where K – the constant dependent on the crystallite shape (0.89); λ – the wavelength of the X-Ray radiation (Cu K_α = 1.54 Å); B – the Full Width at Half Maximum (FWHM or integral breadth) that equals to $((\theta_{High}-\theta_{Low})*\pi)/180$; θ_B – the Bragg angle.

The size distribution and ζ-potential of nanoparticles were measured by DLS from Malvern Instruments Ltd. in the use of a Zetasizer Nano instrument in a prepared buffer solution.[54] Each measurement took 30 s; the particle distribution and electrophoretic curves were obtained by averaging ten measurements. Raman spectra were recorded by using a 3D inverted confocal Raman microscope Confotec NR500 from SOL Instruments Ltd. (Belarusian-Japanese joint venture "SOLAR TII") at 633 nm excitation wavelength with a grating 600gr/mm blazed at 600 nm. The Si wafer with the characteristic Raman line at 520 cm^{-1} was taken as a reference for calibration and basic alignment during integration time from 0.3 to 1 s. The acquired Raman spectra were corrected for the baseline and a background of the Si wafer. A linearly polarized diode laser beam was focused through the objectives with the 100x magnification for Raman spectra acquisition. The laser power was attenuated by using neutral density filters with the following OD values were used 0.6 (25), 0.3 (50) and no filter (100). The molecular structure of nanoparticles (unique fingerprints) was determined by the FTIR Vertex 70 Bruker spectrometer (Germany) in the range from 400 to 4000 cm^{-1} by using the Zeiss Jena Specord-75IR (Germany). A Cary-500 spectrophotometer (Varian, USA) in the wavelength range from 200 to 800 nm was used to acquire the electronic absorption spectra of colloidal solutions.

3. Results and Discussion

As the interface dominates the structure and function of the material, graphene oxide (GO) has been chosen because it provides the extended surface area at the nanoscale that is rich with oxygen containing functional groups such as carboxyl and carbonyl on the edges, and hydroxyl, epoxide groups on the basal plane. GO has amphiphilic properties and its surface is suitable for chemical modification with molecular substances. For this reason we synthesized GO[45,53,54] and used it for the coating of CuO nanoparticles and subsequent functionalization with pristine acetylsalicylic acid (ASA) or diclofenac by ultrasound as shown in **Scheme 1**.

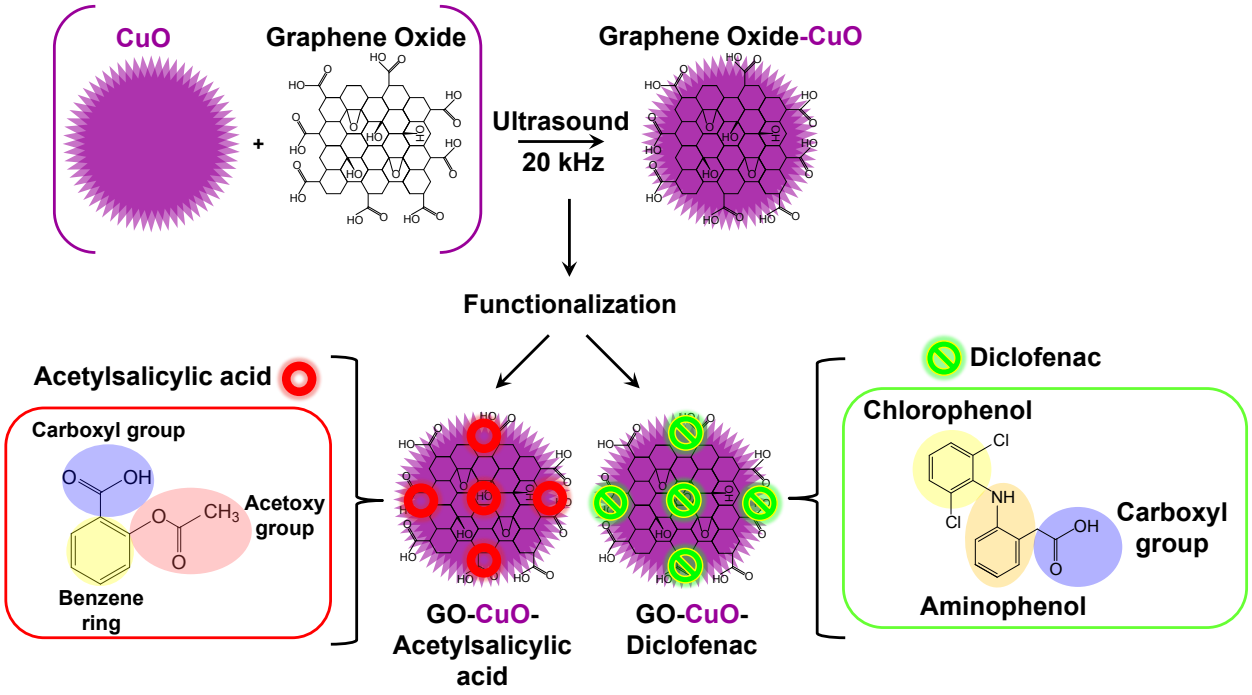

Scheme 1. Formation of graphene oxide-coated CuO nanoparticles by ultrasound (horn-type disperser, 20 kHz, 18 W·cm^{-2}) and subsequent functionalization of pristine nonsteroidal anti-inflammatory drugs: acetylsalicylic acid (ASA) or diclofenac with them.

3.1 Formation of CuO-GO nanoparticles

Representative SEM image shows preformed GO with a sheet-like structure (**Figure 1A**). Dynamic light scattering (DLS) analysis ostends two distinct peaks at ~ 90 ± 37 nm and ~ 455 ± 205 nm in the bimodal size distribution diagram (**Figure 1B**). GO is negatively charged (-22.13 ± 4.62) mV (**Figure 1C**). The ζ-potential magnitude of GO is below the characteristic threshold value ~ -30 mV of a stable colloidal system[58] that can be caused by its lower oxidation degree obtained at mild conditions of ultrasonic treatment resulting in lower amount of ionized acidic groups on GO.[59] Raman spectroscopy reveals two distinct characteristic bands of GO: D line at ~ 1341 cm^{-1} and G line at ~ 1585 cm^{-1} with their intensity ratio as Int_D/Int_G ~ 1.02, indicating that synthesized GO is well crystallized with its low structural defect concentration (**Figure S3**, supporting information). The relatively broadened D band is correlated to a disordering in nanocrystalline carbonaceous dimensions, while its high intensity shows perturbed aromatic rings caused by formation of defects, vacancies and distortions during oxidation. Comparatively narrow G line shows up on localized dimers with sp^2 hybridization or shorter sp^2 chains with a sharper length distribution. The absence of a small peak or a shoulder at ~ 1600-1620 cm^{-1} demonstrates no defects in the crystalline structure of GO induced by substitutional despite the presence of negligible amount of impurities after the synthesis as shown in **Figure S4** and **Table S1** (supporting information). This is important because heteroatoms such as S can replace carbon atoms in the skeleton and break the GO structure in substitutional doping. Disordering in synthesized GO can be induced by surface transfer doping that doesn't destroy the chemical bonds of this material. Second order Raman bands of GO appear near 2682 cm^{-1} and 2926 cm^{-1} that can be assigned to 2D and {D+G} overtones observed in defect-free GO with induced disorder due to oxidation. The relatively broad feature of these two bands reveals the presence of a small portion of amorphous carbon with sp^3 hybridization. Therefore we can

assume that the structure of synthesized GO would enable functionalization of ASA or diclofenac through the surface transfer interactions with oxygen functional groups.

The ultrasonically formed GO-CuO nanoparticles have a flower-like morphology consisting of twisted thin sheets with a specific orientation as a result of the growth in a perpendicular direction to the surface of the initial nucleation units, i.e. $[Cu(OH)_4]^{2-}$ (**Figure 1D**). The DLS diagram exhibits a unimodal size distribution with a single peak at ~342 ± 160 nm (**Figure 1E**). The surface charge has a positive ζ-potential of 2.57 ± 1.13 mV, that is in agreement with CuO nanoparticles at pH = 7-9 and is indicative of the isoelectric point of CuO nanoparticles in aqueous solution at pH = 5.42[60] (**Figure 1F**). As next, we examined the electronic molecular structure of GO and GO-CuO by using the UV-Vis absorption spectra (**Figure 1G**). GO exhibits a strong narrow absorption band at 243 nm (5.10 eV) because of the π–π* transition of aromatic C=C bonds and a smaller broader peak at 320 nm (3.88 eV) as a result of the n–π* transition of C=O bonds. In contrast to GO, the absorption spectrum of GO-CuO nanoparticles is more complex and exhibits multiple peaks with most prominent maxima at 268 nm (4.63 eV), 335 nm (3.70 eV) and a very strong band at 744 nm (1.67 eV).

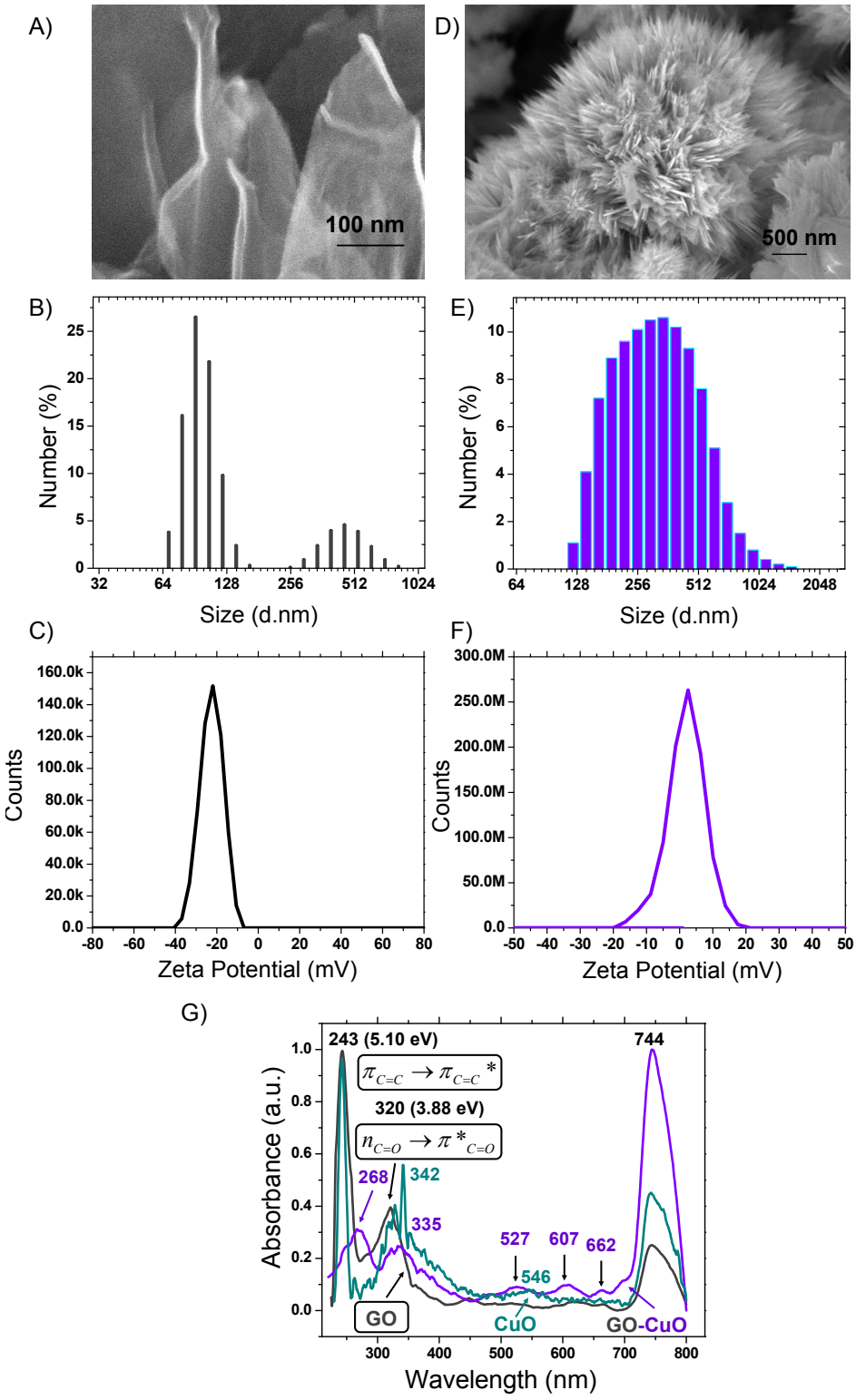

Figure 1. Representative SEM images of A) synthesized graphene oxide (GO) and D) ultrasonically formed GO-coated CuO nanoparticles. DLS size distribution diagrams of B) GO

and E) GO-coated CuO nanoparticles. Zeta potential plots of C) GO and F) GO-coated CuO nanoparticles. G) UV-Vis absorption spectra of GO and GO-coated CuO nanoparticles in aqueous solution.

In Figure 1G 268 nm and 335 nm absorption peaks are red shifted in comparison to the common absorption band of GO (220 - 230 nm and a shoulder near 300 – 303 nm), indicating a restored electronic conjugation within the graphene sheets.[61] An absorption band near 744 nm is attributed to the electronic excitation of solvent molecules.[62] The first absorption peak in the CuO-GO nanocomposite is red shifted, indicating a reduction of GO. The second absorption peak together with other small bands at 527 nm (2.35 eV), 607 nm (2.04 eV) and 662 nm (1.87 eV) can be assigned to the band-to-band transition in a flower-like morphology of GO-coated CuO nanoparticles based on the observation of similar n–π^* transitions in CuO nanoparticles with a sisal-like morphology due to a quantum confinement in radial direction of nanoneedle structures.[63]

3.2 The crystalline structure of CuO-GO nanoparticles

The phase composition of GO and GO-coated CuO nanoparticles was defined by the X-ray powder diffraction technique (**Figure 2A** and **B**). The XRD pattern of GO shows an intense strong peak at 2θ = 12.66 that corresponds to the interplanar spacing *d* of 5.83 Å (**Table S2**, supporting information). This *d* value is ~ 1.44 Å larger than of a (001) reflex in diamond (amcsd 0013983). Another XRD peak of GO is broad and has a lower intensity with a maximum at 2θ = 22.84 corresponding to *d* of 3.96 Å that is closer to the *d* value of (002) reflex in graphite (amcsd 0000049) at 2θ = 26.63 (d = 3.34 Å). Other four narrow sharp peaks of GO appear on the amorphous halo at 2θ = 35.06, 38.30, 40.05 and 42.87 and have the *d* values of 2.53 Å, 2.60 Å, 2.49 Å and 2.33 Å that are larger than of (111), (020), (021) and (201) reflexes in diamond.

These changes of XRD reflexes point out to the thinning of graphite sheets and a disordered stacking of graphene layers enriched with oxygen functional groups. The mechanical shock waves and shear forces, arising in cavitation hot spots, can cause exfoliation and deformation of GO leading to its amorphization.[64]

The XRD pattern of sonochemically synthesized GO-coated CuO nanoparticles shows characteristic reflexes of CuO crystalline phase (amcsd 0018812). However, the calculated *d* values of GO-coated CuO nanoparticles with (110), (111), (020) and (202) planes are on 0.1 Å larger than in CuO (**Table S3**, supporting information). In addition, the (112) reflex of CuO in GO-coated CuO nanoparticles has a larger *d* value of 1.81 Å than in CuO (1.77 Å). The overall broadening of reflexes is indicative for the presence of oxidized graphene and formation of oxygen-containing functional groups in metal oxides in the sonochemically modified GO with CuO nanoparticles, in agreement with the proposed sonochemical formation mechanism.[65] However, small (200) reflex of GO-coated CuO at $2\theta = 43.28$ has a decreased *d* value of 2.07 Å that is on 0.24 Å smaller than in CuO nanoparticles, pointing out to the coating of CuO with GO through the binding with C-O or C=O functional groups.

In a control experiment, in which the mixture of preformed CuO nanoparticles and GO was ultrasonically treated (20 kHz, 18 $W \cdot cm^{-2}$, 15 min), the XRD pattern reveals (001) and (002) planes of GO, (002) and (111) planes of CuO, and strong (111), (200) and (220) planes of Cu (**Figure 2C**). Among them the dominant XRD peaks arise from GO and Cu, demonstrating the copper in a zerovalent state in GO as a result of sonochemical redox reactions involving electron transfer from copper cations to carbon and oxygen through the interaction with -OH and -COOH groups during acoustic cavitation.[66] This sonochemically formed{CuO+GO} colloidal mixture

has a completely different structure than GO-coated CuO nanoparticles that are entirely composed of a pure CuO phase and a carbonaceous network of graphene oxide.

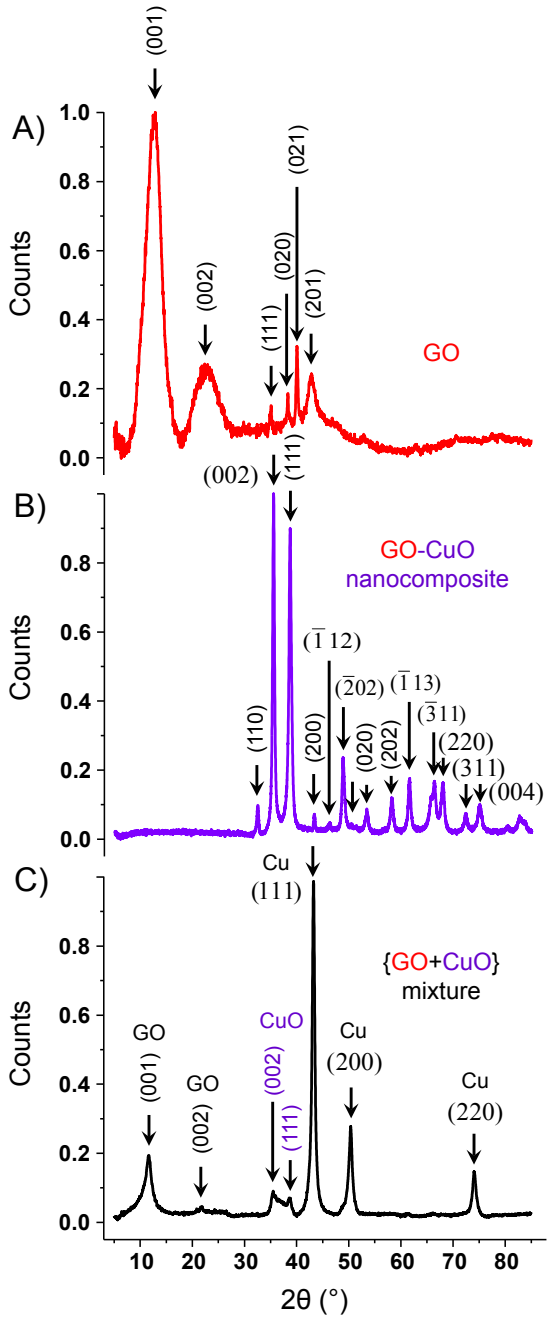

Figure 2. X-Ray powder diffraction patterns of (A) preformed GO, (B) ultrasonically synthesized GO-coated CuO nanoparticles and (C) sonochemically formed{CuO+GO} colloidal mixture (20 kHz, 18 W·cm^{-2}, 15 min).

The elemental composition of GO-coated CuO nanocomposites was determined from EDX spectra and compared to the sonochemically formed {CuO+GO} colloidal mixture (**Figure S5** and **Table S4**, supporting information). GO-coated CuO nanocomposites are composed of C (~ 51.2 atom.%), O (~ 36.8 atom.%) and Cu (~ 12.0 atom.%) (**Figure S5A**, supporting information). For comparison, the carbon concentration in GO (C ~ 59.2 atom.%) **(Figure S4** and **Table S1**, supporting information) is higher than in GO-coated CuO nanocomposites, but comparable to the {CuO+GO} mixture (C ~ 59.6 atom.%) (**Figure S5B** and **Table S4**, supporting information). The oxygen concentration in GO (O ~ 39.7 atom.%) is higher than in GO-coated CuO nanocomposites, but much lower in the {CuO+GO} mixture (O ~ 30.8 atom.%) that contains Cu (~ 8.6 atom.%), and this is in agreement with the identified sonochemically formed zerovalent Cu (**Figure 2C**).

3.3 The electronic molecular structure of ASA-CuO-GO and diclofenac-CuO-GO

The synthesized GO-coated CuO nanocomposites were used to functionalize pristine ASA or diclofenac by ultrasound. The molecular chemical structure and complexation of ASA or diclofenac with GO-coated CuO nanocomposites was defined by the FTIR transmittance spectroscopy and compared to pristine drugs (**Figure 3**). FTIR spectra of ASA-GO-coated CuO or diclofenac-GO-coated CuO nanoparticles show characteristic peaks of Cu-O vibration[67] at 485 cm^{-1} (**Table S5**, supporting information) and at 537 cm^{-1} (**Table S6**, supporting information), pointing out to different binding mechanisms of ASA or diclofenac to the GO-coated CuO surface caused by the changes in the electronic configuration of the neighboring functional groups. The closest bands to the Cu-O vibration are the C-H out of plane ring bending of ASA (~ 702 cm^{-1}), C-H vibration of the methyl group and the C=O-OH stretching of the carboxylic group due to the interaction with the Cu-O-H in ASA-GO-coated CuO nanoparticles

(**Figure 3A**). The ultrasonic binding of diclofenac to GO-coated CuO nanoparticles can occur involving interaction with the Cu-O and C-H benzene ring (~ 664-853 and 1025 cm^{-1}) as indicated by their strong bands, but also through the C=C-OH bonding and interaction with –C=O carboxylic groups (~ 900 and 1160 cm^{-1}), and C-Cl (to a much lesser degree) (**Figure 3C**). The binding of both NSAIDs can also involve their interaction with the –C=O carboxylic moiety through the formation of the internal H-bonding: band at 1650 cm^{-1} in ASA-GO-CuO and at 1638 cm^{-1} in diclofenac-GO-CuO.

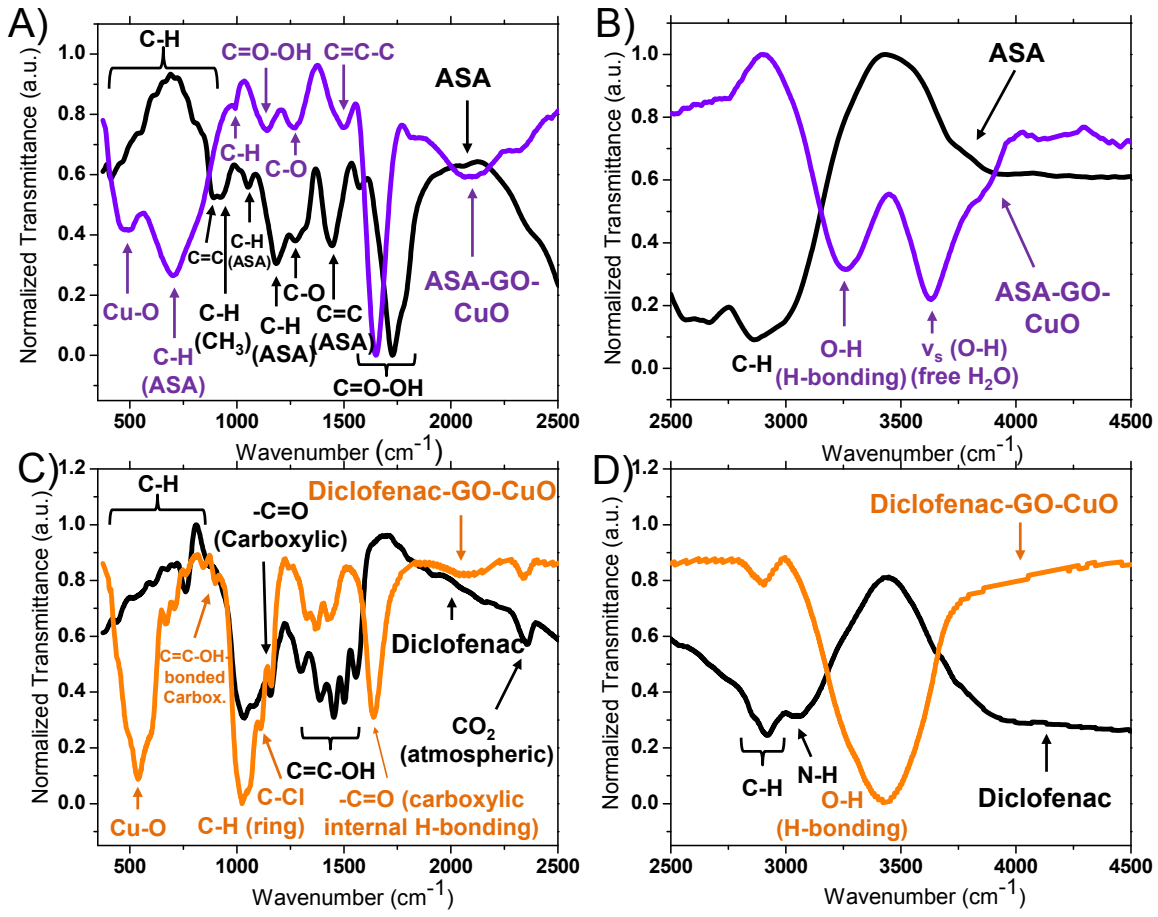

Figure 3. Fourier transform infrared transmittance spectra of (A and B) ASA-GO-coated CuO and (C and D) diclofenac-GO-coated CuO nanocomposites. FTIR spectra of pristine ASA and diclofenac are shown for comparison.

The presence of H-bonding is identified by the appearance of a broad band at 3260 cm^{-1} in ASA-GO-coated CuO (**Figure 3B**) and at 3435 cm^{-1} in diclofenac-GO-coated CuO nanocomposites (**Figure 3D**). In contrast to diclofenac, the O-H stretching of free water molecules at 3632 cm^{-1} in ASA-GO-CuO can be associated to CuO.[68] The next question to answer was, whether CuO and GO can prevent the drug from undesirable surface defects or damage caused by ultrasound. To find it out, pristine ASA or diclofenac (in a powder form) were treated by ultrasound (20 kHz, 18 $W \cdot cm^{-2}$) in deionized water (pH = 5.5) for 1, 3, 5, 10, 15 or 30 min. To note, we were able to collect the powders of ASA treated only up to 15 min and had to terminate sonication because of its complete dissolution in aqueous solution. In contrast to ASA, sonication of diclofenac (powder) in aqueous solution for 30 min did not result in its entire dissolution enabling us to collect the sediment and use it for the study by FTIR spectroscopy.

Overall, FTIR spectra of pristine ASA and diclofenac after 1-15 min of sonication are similar to those of untreated powder, demonstrating that ultrasound did not changed the chemical structure of these drugs (**Figure S6** and **S7**, **Table S7** and **S8**, supporting information). However, considerable changes in spectra were observed in diclofenac after 30 min of ultrasonic treatment. In particular, multiple peaks were replaced by two small C-H bands of diclofenac (440 and 675 cm^{-1}) and C-Cl vibration (1108 cm^{-1}) disappeared (**Table S8**, supporting information). In addition, the C-H vibration in the far infrared region splitted into two peaks at 2853 and 2917 cm^{-1} and the disappearance of the N-H stretching (3245 cm^{-1}) was accompanied by the appearance of a strong broad OH band (3463 cm^{-1}), indicating the H-bond formation between the disrupted benzene rings of diclofenac.

It is important to note, that the C=C-OH vibration of the carboxylic acid group in diclofenac remained unchanged at 900 cm^{-1}, but disappeared at 1367 cm^{-1}, while the –C=O band of this

group was blue shifted at 1153 cm^{-1} and disappeared at 1640 cm^{-1}, indicating the loss of the internal H-bonding involving the C=O carboxylic acid groups after 30 min of sonication. However, three small C=O bands of carbonyl group in diclofenac appeared at 1725, 1796 and 1845 cm^{-1} after 30 min of sonication demonstrating that H-bonding mostly involves the C-H vibrational bands of one of the benzene rings and carbonyl groups instead of the C-Cl and carboxylic acid moieties. In general, ultrasound caused the scissoring of two benzene rings and a significant loss of the carboxylic acid groups and C-Cl moiety in pristine diclofenac, but preserved C=O carbonyl groups that were interconnected by H-bonds. Therefore we can assume that ultrasound binds diclofenac through the Cu-O bond formation with the C-H benzene ring and –C=O carboxylic acid moieties with the internal H-bonding in the presence of GO-coated CuO nanoparticles.

3.4 The stability of ASA-CuO-GO and diclofenac-CuO-GO at pH = 1, 5 or 8 in water

The interaction of ASA-GO-coated CuO and diclofenac-GO-coated CuO nanocomposites with the UV-Visible radiation was examined in order to identify ASA molecules and its hydrolysis products, diclofenac and its polyatomic species, including ions and complexes with CuO, GO and GO-CuO (**Figure S8** and **S9**, supporting information). The stability of nanocomposites was explored by the UV-Vis absorption spectroscopy in aqueous solutions adjusted to pH = 1, 5 or 8 (**Figure 4**). The UV-Vis absorption spectrum of pristine ASA aqueous solution shows two absorption maxima at 237 and 296 nm (**Figure S8**, supporting information). The first absorption peak (5.23 eV) can be assigned to the singlet transition in the π (bonding) molecular orbital from the phenyl ring involving –C=C- or C=O bonds to its π* (anti-bonding) orbital and is designated as $^1(\pi_{py}\text{-}\pi_{co}^*)$ of ASA.[68] The π-π^* transition typically occurs in a molecule that possesses a chromophore with an unsaturated bond such as C=C or C=O in the

carboxylic acid. The second absorption peak (4.19 eV) results from the singlet transition in electronically excited oxygen lone pair of the *n* (non-bonding) atomic orbital of the -C-OH bond to the π^* (anti-bonding) orbital and is designated as $^1(n_o\text{-}\pi_{co}^*)$ of the salicylic acid.[68]

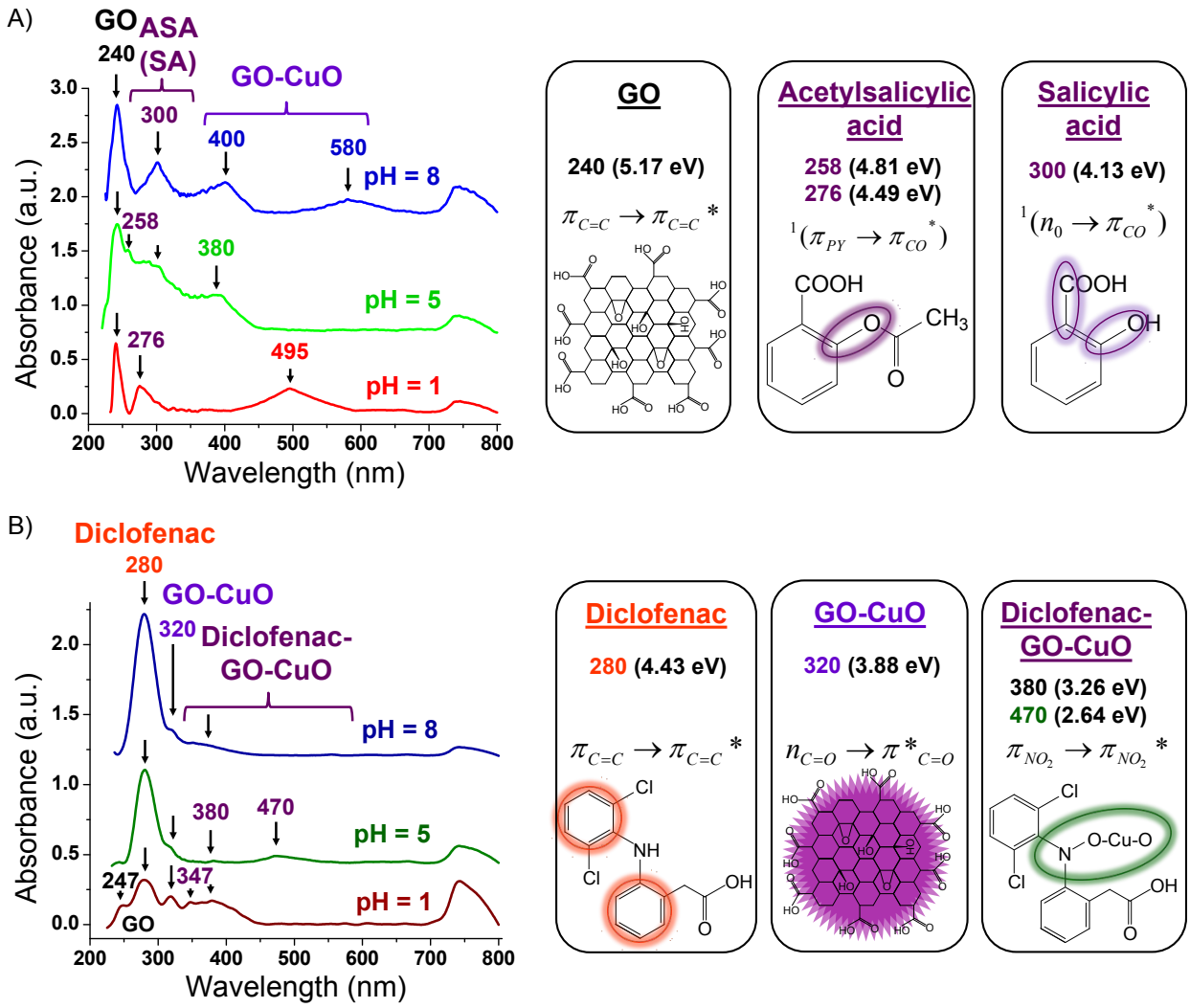

Figure 4. UV-Vis absorption spectra of A) ASA-GO-coated CuO and B) diclofenac-GO-coated CuO nanocomposites after incubation in aqueous solution at pH = 1, 5 or 8.

The binding of ASA to GO transformed the peak at 237 nm into a shoulder of an intense absorption band at 227 nm of GO due to the π–π^* transition in aromatic C=C bonds as confirmed by the calculated triplet electronic transition, demonstrating the conjugation of this drug with

GO. The absorption peak of salicylic acid at 296 nm appeared as a broad peak with a maximum at 276 nm that is a characteristic band of ASA. These changes in the absorption spectra were followed by the appearance of a small peak near 336 nm (3.69 eV) due to the C=O band-to-band n_o-π_{co}* transition in GO. In contrast to GO, the binding of ASA to GO-CuO occurs via the n-π* transition in the C=O band of GO. Its closer junction to CuO (330 nm) takes place through the singlet electronic transition of the acetyl-carbonyl group (341 nm) involving interaction with the salicylic acid moiety of the second derivative (296 nm) component. These observations are in agreement with the FTIR analysis.

It is important to note, that the electronic molecular structure of ASA-GO-coated CuO nanocomposites changed at pH = 1, 5 or 8 (**Figure 4A**).UV-Vis absorption spectra of these nanocomposites exhibited an intense peak of GO at 240 nm at any pH. At pH = 1 a single absorption peak of ASA at 276 nm reveals that the drug (~ 99%) is in its nonionized form. Therefore ASA-GO-coated CuO nanocomposites can be potentially able of diffusing through the lipid membrane in the stomach acidic medium. Another very broad absorption band (~ 495 nm) appeared at pH = 1, pointing out to the closer junction of ASA to the sisal-like CuO nanoparticle with a typical band closer to GO (~ 2.27eV). At pH = 5, the main absorption peak of ASA (276 nm) appeared as a broad band with small maxima at 258 nm (4.81 eV) and 400 nm (3.1 eV). These changes demonstrate the gradual ionization of ASA in contact with the carboxylic and salicylic acid groups and CuO with a nanoplatelet morphology, which has a characteristic absorption band at 400 nm. At pH = 8, three broad absorption maxima (300, 400 and 580 nm) appeared in addition to the previously mentioned GO peak at 240 nm. These peaks point out to the dissolution of ASA from GO-coated CuO nanocomposites in basic medium,

leaving the salicylic acid moiety as the hydrolysis product in the closer junction with the GO-CuO surface.

In contrast to ASA, the UV-Vis absorption spectrum of pristine diclofenac showed only one band at 278 nm (4.46 eV) as a result of π–π* transition in aromatic C=C bonds, and the position of this band was not influenced by the binding of diclofenac to GO or GO-coated CuO nanocomposite[69] (**Figure S9**, supporting information). The UV-Vis absorption spectra of diclofenac-GO and diclofenac-GO-coated CuO nanocomposite exhibit a small peak at 333 nm (3.72 eV) pointing out to the band-to-band transition in GO. Another two broad weak peaks near 432 and 456 nm can be assigned to diclofenac with the structure comparable to the O-nitro aniline depending on its oxidation state.[69]

The absorption spectra of diclofenac-GO-coated CuO nanocomposites in aqueous solution adjusted to pH = 1, 5 or 8 are shown in **Figure 4B**. It is established that diclofenac undergoes the intramolecular cyclization in acidic medium leading to inactivation of this drug.[69] In contrast, at pH = 1, diclofenac-GO-coated CuO nanocomposites exhibit a complicated UV-Vis absorption spectrum that shows multiple peaks with a maximum at 247 nm (5.02 eV) due to the interaction with GO. In this absorption spectrum a broad peak at 280 nm (4.43 eV) that is assigned to diclofenac appears with a lower intensity because the drug loses Na^+ and becomes less soluble as only Na^+ favors its dissolution in H_2O.[69] The presence of a smaller band at 320 nm points out to the binding of diclofenac to the GO-coated CuO nanoparticle. Another important feature is a broad band with distinct maxima near 347 and 380 nm that are located in the absorption region of n–π* transition in GO-coated CuO nanoparticles and π–π* transition in NO_2 group of aniline's phenyl ring of diclofenac.[69] At pH = 5, all these peaks became weaker except of the main absorption band of diclofenac (280 nm) and a very small peak appeared near 470 nm pointing

out to the formation of Cu-8-quinolinate in H_2O.[70] At pH = 8, the characteristic absorption peak of diclofenac became more pronounced but without any spectral shift. Other bands (320 nm, 347 nm and 740 nm) appeared with a decreased intensity, while the band near 380 nm disappeared, demonstrating a lower amount of diclofenac molecules in GO-coated CuO nanocomposite in basic medium.

In our experiments, CuO-GO nanoparticles have a relatively large average size (342 ± 160 nm) and well-defined flower-like morphology, CuO crystalline phase and amphiphilic GO coating in the complex with ASA or diclofenac that would be beneficial for intracellular studies because of the following reasons. This large size and well-defined spherical morphology of CuO would induce less toxicity to mammalian cells. The possible cytotoxicity caused by ROS production and copper ion leaching of CuO-GO NPs could be controlled by the specific interaction with ASA or diclofenac and functional groups of GO. The bioavailability of ASA or diclofenac together with GO would also contribute to the reduction of possible toxic effects in mammalian cells, and can profitably enhance antibacterial action in bacteria. For more reliable *in vivo* studies the size of ASA-CuO-GO and diclofenac-CuO-GO nanocomposite should be decreased to 100 nm or lower.

4. Conclusions

A feasible single step method was demonstrated for the design of GO-coated CuO nanoparticles with a flower-like morphology by ultrasound (20 kHz, 18 $W \cdot cm^{-2}$). These nanoparticles are positively charged and composed of GO with a pure CuO phase. We also introduced how ultrasound can be applied for functionalization of pristine acetylsalicylic acid (ASA) or diclofenac with these nanoparticles in a simple manner. In this approach ultrasound binds free ASA to GO-coated CuO nanoparticles through the complexation with Cu-O, C-H of

the benzene ring and carboxylic acid moiety that are linked with H-bonds, as determined by the UV-Vis absorption and FTIR spectroscopy methods. In contrast, ultrasonic complexation of diclofenac with GO-coated CuO nanoparticles takes place with the C-H bond in one of its isolated benzene rings and carbonyl groups (instead of C-Cl bond) and involves carboxylic groups of GO in the H-bonded network. Both ASA-GO-CuO and diclofenac-GO-CuO nanocomposites are linked with H-bonds within the CuO-GO complex. As the aqueous medium becomes more basic, ASA undergoes hydrolysis and its active component (salicylic acid) is retained in GO-coated CuO nanoparticles within the H-bonded network. In contrast, diclofenac is strongly bonded with GO-coated CuO nanoparticles and remains stable at higher pH values due to complexation.

This new knowledge improves our understanding about the electronic molecular structure of acetylsalicylic acid (ASA) and salicylic acid (SA) as well as diclofenac and their ionization states during interaction with CuO nanoparticles and oxidized graphene that can be expanded to many other drugs. New findings can be of use for the fundamental studies of the intracellular drug-enzyme functions especially in *in vivo* application.

ASSOCIATED CONTENT

Supporting Information.

The following files are available free of charge.

Synthesis of GO; calibration of N.4-20 ultrasonic disperser (20 kHz, Cavitation Inc., Republic of Belarus); Raman spectrum of GO; X-Ray powder diffraction patterns and Energy Dispersive X-Ray fluorescence spectra of GO, CuO and GO-coated CuO nanoparticles; FTIR transmittance and UV-Vis absorption spectra of pristine ASA and diclofenac, ASA-GO and diclofenac-GO nanoparticles, ASA-GO-coated CuO and diclofenac-GO-coated CuO nanocomposites in aqueous solutions.

AUTHOR INFORMATION

Corresponding Author

*Darya Radziuk, E-mail: radziuk@bsuir.by

Author Contributions

The manuscript was written through contributions of all authors. All authors have given approval to the final version of the manuscript.

Funding Sources

This work is supported by the BRFFR grant № 16-3041 57 031.00 and MOST Belarus-EU financial program through grants № R-YPQZ-53145 and 57111R-dDMu-57100.

ACKNOWLEDGMENT

Prof. Mikhail Artemyev and Prof. Ludmila Ivashkevich from the Belarusian State University (Minsk) gratefully acknowledged for the ZP/DLS, XRD measurements and constructive

discussions. We appreciate Dr. A.G. Karoza from B.I. Stepanov Institute of Physics of National Academy of Sciences (Republic of Belarus) for the spectroscopy measurements and consultation.

REFERENCES

1. Patrono, C.; Baigent,C. Role of aspirin in primary prevention of cardiovascular disease. *Nat. Rev. Cardiol.*, **2019**, *16*, 675-686.

2. Maniar, K. H.; Jones, I. A.; Vangsness, C. T.; Gopalakrishna, R. Lowering side effects of NSAID usage in osteoarthritis: recent attempts at minimizing dosage. *Expert Opin. Pharmacother.*, **2018**, *19*, 93-102.

3. Drew, D. A.; Cao, Y.; Chan, A. T. Aspirin and colorectal cancer: the promise of precision chemoprevention. *Nat. Rev. Cancer*, **2016**, *16*, 173-186.

4. Zhao, Q.; Dai, C.; Fan, S.; Lv, J.; Nie, L. Synergistic efficacy of salicylic acid with a penetration enhancer on human skin monitored by OCT and diffuse reflectance spectroscopy *Sci. Rep*., **2016**, *6*, 34954.

5. Lima Silva, C. C.; Shimo, H. M.; de Felício, R.; Mercaldi, G. F.; Rocco, S. A.; Benedetti, C. E. Structure-function relationship of a citrus salicylate methylesterase and role of salicylic acid in citrus canker resistance. *Sci. Rep.*, **2019**, *9*, 3901.

6. Hua, H.; Zhang, H.; Kong, Q.; Wang, J.; Jiang, Y. Complex roles of the old drug aspirin in cancer chemoprevention and therapy. *Med. Res. Rev.*, **2019**, *39*, 114-145.

7. Ornelas, A.; Zacharias-Millward, N.; Davis, J. S.; Lichtenberger, L.; Hawke, D.; Hawk, E.; Vilar, E.; Bhattacharya, P.; Millward, S. Beyond COX-1: the effects of aspirin on

platelet biology and potential mechanisms of chemoprevention. *Cancer Metastasis Rev.*, **2017**, *36*, 289-303.

8. Schmidt, M.; Sørensen, H. T.; Pedersen, L. Diclofenac use and cardiovascular risks: series of nationwide cohort studies. *BMJ*, **2018**, *362*, k3426.

9. a) Bjarnason, I.; Scarpignato, C.; Holmgren, E.; Olszewski, M.; Rainsford, K. D.; Lanas, A. Mechanisms of Damage to the Gastrointestinal Tract from Nonsteroidal Anti-Inflammatory Drugs. *Gastroenterology,* **2018**, *154*, 500-514; b) García-Rayado, G.; Navarro, M.; Lanas, A. NSAID induced gastrointestinal damage and designing GI-sparing NSAIDs. *Expert. Rev. Clin. Pharmacol.*, **2018**, *11*, 1031-1043; c) Sodeifian, G.; Razmimanesh, F. Diffusional interaction behavior of NSAIDs in lipid bilayer membrane using molecular dynamics (MD) simulation: aspirin and ibuprofen. *J Biomol. Struct. Dyn*., **2019**, *37*, 1666-1684; d)) Goldstein, J. L.; Cryer, B. Gastrointestinal injury associated with NSAID use: a case study and review of risk factors and preventative strategies. *Drug, Healthcare and Patient Safety* **2015**, *7*, 31-41; e) Aspirin Product Monograph, Submission Control No: 202259, Bayer Inc. **2014**; f) Rainsford, K. D. Ibuprofen: pharmacology, efficacy and safety. *Inflammopharmacol.*, **2009**, 17, 275-342.

10. Levina, E. O.; Penkov, N. V.; Rodionova, N. N.; Tarasov, S. A.; Barykina, D. V.; Vener, M. V. Hydration of the carboxylate group in anti-inflammatory drugs: ATR-IR and computational studies of aqueous solution of sodium diclofenac. *ACS Omega*, **2018**, *3*, 302-313.

11. Singh, S. K.; Joshi, P. R.; Shaw, R. A.; Hill, J. G.; Das, A. Interplay between hydrogen bonding and n→π* interaction in an analgesic drug salicin. *Phys. Chem. Chem. Phys*., **2018**, *20*, 18361-18373.

12. Bende, G.; Biswal, S.; Bhad, P.; Chen, Y.; Salunke, A.; Winter, S.; Wagner, R.; Sunkara, G. Relative bioavailability of diclofenac potassium from softgel capsule versus powder for oral solution and immediate-release tablet formulation. *Clin. Pharm. Drug Dev*., **2016**, *5*, 76-82.

13. Xu, M.; Heng, P. W. S.; Liew, C. V. Formulation and process strategies to minimize coat damage for compaction of coated pellets in a rotary tablet press: a mechanistic view. *Int. J Pharm.*, **2016**, *499*, 29-37.

14. Elwerfalli, A. M.; Ghanchi, Z.; Rashid, F.; Alany, R. G.; ElShaer, A. New generation of orally disintegrating tablets for sustained drug release: a propitious outlook. *Curr. Drug Deliv.*, **2015**, *12*, 652-667.

15. Francio, V. T.; Davani, S.; Towery, C.; Brown, T. L. Oral versus topical diclofenac sodium in the treatment of osteoarthritis. *J Pain Palliat. Care Pharmacother*., **2017**, *31*, 113-120.

16. Banti, C. N.; Hadjikakou, S. K. Non-steroidal anti-inflammatory drugs (NSAIDs) in metal complexes and their effect at the cellular level. *Eur. J. Inorg. Chem.*, **2016**, *2016*, 3048-3071.

17. Leung, C.-H.; Lin, S.; Zhong, H.-J.; Ma, D.-L. Metal complexes as potential modulators of inflammatory and autoimmune responses. *Chem. Sci.*, **2015**, *6*, 871-884.

18. Lo, K. K.-W. (Ed.); Inorganic and organometallic transition metal complexes with biological molecules and living cells; Academic Press, Hong Kong, **2017**, pp. 406.

19. Banti, C. N.; Papatriantafyllopoulou, C.; Tasiopoulos, A. J.; Hadjikakou, S. K. New metalo-therapeutics of NSAIDs against human breast cancer cells. *Eur. J Med Chem.*, **2018**, *143*, 1687-1701.

20. Pettenuzzo, A.; Pigot, R.; Ronconi, L. Metal-based glycoconjugates and their potential in targeted anticancer chemotherapy. *Metallodrugs*, **2015**, *1*, 36-61.

21. Sun, Y.; Heidary, D. K.; Zhang, Z.; Richards, C. I.; Glazer, E. C. Bacterial cytological profiling reveals the mechanism of action of anticancer metal complexes. *Mol. Pharmaceutics*, **2018**, *15*, 3404-3416.

22. Simunkova, M.; Lauro, P.; Jomova, K.; Hudecova, L.; Danko, M.; Alwasel, S.; Alhazza, I. M.; Rajcaniova, S.; Kozovska, Z.; Kucerova, L.; Moncol, J.; Svorc, L.; Valko, M. Redox-cycling and intercalating properties of novel mixed copper(II) complexes with non-steroidal anti-inflammatory drugs tolfenamic, mefenamic and flufenamic acids and phenanthroline functionality: Structure, SOD-mimetic activity, interaction with albumin, DNA damage study and anticancer activity. *J. Inorg. Biochem*., **2019**, *194*, 97-113.

23. Hussain, A.; AlAjmi, M. F.; Rehman, Md. T.; Amir, S.; Husain, F. M.; Alsalme, A.; Siddiqui, M. A.; AlKhedhairy, A. A.; Khan, R. A. Copper(II) complexes as potential anticancer and Nonsteroidal anti-inflammatory agents: In vitro and in vivo studies. *Sci. Rep.*, **2019**, *9*, 5237.

24. Leung, C.-H.; Lin, S.; Zhong, H.-J.; Ma, D.-L. Metal complexes as potential modulators of inflammatory and autoimmune responses. *Chem. Sci.*, **2015**, *6*, 871-884.

25. Krstić, N. S.; Nikolić, R. S.; Stanković, M. N.; Nikolić, N. G.; Dorđević, D. M. Coordination compounds of M(II) biometal ions with acid-type anti-inflammatory drugs as ligands - a review. *Trop. J. Pharm. Res.*, **2015**, *14*, 337-349.

26. Lu, C.; Laws, K.; Eskandari, A.; Suntharalingam, K. A reactive oxygen species-generating, cyclooxygenase-2 inhibiting, cancer stem cell-potent tetranuclear copper(II) cluster. *Dalton Trans.*, **2017**, *46*, 12785-12789.

27. Eskandaria, A.; Suntharalingam, K. A reactive oxygen species-generating, cancer stem cell-potent manganese(II) complex and its encapsulation into polymeric nanoparticles. *Chem. Sci.*, **2019**, *10*, 7792-7800.

28. Bennett, J. S. Novel platelet inhibitors. *Annu. Rev. Med*., **2001**, *52*, 161-184.

29. Weder, J. E.; Dillon, C. T.; Hambley, T. W.; Kennedy, B. J.; Lay, P. A.; Biffin, J. R.; Regtop, H. L.; Davies, N. M. Copper complexes of nonsteroidal anti-inflammatory drugs: an opportunity yet to be realized. *Coord. Chem. Rev*., **2002**, *232*, 95.

30. Berry, D. J.; Steed, J. W. Pharmaceutical cocrystals, salts and multicomponent systems; intermolecular interactions and property based design. *Adv. Drug Delivery Rev.*, **2017**, *117*, 3-24.

31. García-Rayado, G.; Navarro, M.; Lanas, A. NSAID induced gastrointestinal damage and designing GI-sparing NSAIDs. *Expert. Rev. Clin. Pharmacol*., **2018**, *11*, 1031-1043.

32. Sodeifian, G.; Razmimanesh, F. Diffusional interaction behavior of NSAIDs in lipid bilayer membrane using molecular dynamics (MD) simulation: aspirin and ibuprofen. *J Biomol. Struct. Dyn.,* **2019**, *37*, 1666-1684.

33. Lipinski, C. A.; Lombardo, F.; Dominy, B. W.; Feeney, P. J. Experimental and computational approaches to estimate solubility and permeability in drug discovery and development settings. *Adv. Drug Delivery Rev*., **2001**, *46*, 3-26.

34. Zhao, S.; Caruso, F.; Dähne, L.; Decher, G.; De Geest, B. G.; Fan, J.; Feliu, N.; Gogotsi, Y.; Hammond, P. T.; Hersam, M. C.; Khademhosseini, A.; Kotov, N.; Leporatti, S.; Li, Y.; Lisdat, F.; Liz-Marzán, L. M.; Moya, S.; Mulvaney, P.; Rogach, A. L.; Roy, S.; Shchukin, D. G.; Skirtach, A. G.; Stevens, M. M.; Sukhorukov, G. B.; Weiss, P. S.; Yue, Z.; Zhu, D.; Parak, W. J. The future of Layer-by-Layer assembly: a tribute to ACS Nano associate editor Helmuth Möhwald. *ACS Nano*, **2019**, *13*, 6151-6169.

35. Martín, C.; Kostarelos, K.; Prato, M.; Bianco, A. Biocompatibility and biodegradability of 2D materials: graphene and beyond. *Chem. Commun*., **2019**, *55*, 5540-5546.

36. Guarnieri, D.; Sánchez-Moreno, P.; Del Rio Castillo, A. E.; Bonaccorso, F.; Gatto, F.; Bardi, G.; Martín, C.; Vázquez, E.; Catelani, T.; Sabella, S.; Pompa, P. P. Biotransformation and biological interaction of graphene and graphene oxide during simulated oral ingestion. *Small*, **2018**, *14*, e1800227.

37. Sengupta, I.; Bhattacharya, P.; Talukdar, M.; Neogi, S.; Pal, S. K.; Chakraborty, S. Bactericidal effect of graphene oxide and reduced graphene oxide: influence of shape of bacteria. *Colloids Interface Sci. Commun.*, **2019**, *28*, 60-68.

38. Fadeel, B.; Bussy, C.; Merino, S.; Vázquez, E.; Flahaut, E.; Mouchet, F.; Evariste, L.; Gauthier, L.; Koivisto, A. J.; Vogel, U.; Martin, C.; Delogu, L. G.; Bürki-Thurnherr, T.; Wick, P.; Beloin-Saint-Pierre, D.; Hischier, R.; Pelin, M.; Carniel, F. C.; Tretiach, M.; Cesca, F.; Benfenati, F.; Scaini, D.; Ballerini, L.; Kostarelos, K.; Prato, M.; Bianco, A. Safety assessment of graphene-based materials: focus on human health and the environment. *ACS Nano*, **2018**, *12*, 10582-10620.

39. Nishino, F.; Jeem, M.; Zhang, L.; Okamoto, K.; Okabe, S.; Watanabe, S. Formation of CuO nano-flowered surfaces via submerged photo-synthesis of crystallites and their antimicrobial activity. *Sci. Rep*., **2017**, *7*, 1063.

40. Boltaev, G. S.; Ganeev, R. A.; Krishnendu, P. S.; Zhang, K.; Guo, C. Nonlinear optical characterization of copper oxide nanoellipsoids. *Sci. Rep*., **2019**, *9*, 11414.

41. Deng, Z.; Ma, Z.; Li, Y.; Li, Y.; Chen, L.; Yang, X.; Wang, H.-E.; Su, B.-L. Boosting lithium-ion storage capability in CuO nanosheets via synergistic engineering of defects and pores. *Front. Chem.*, **2018**, *6*, 1-9.

42. Naatz, H.; Lin, S.; Li, R.; Jiang, W.; Ji, Z.; Chang, C. H.; Köser, J.; Thöming, J.; Xia, T.; Nel, A. E.; Mädler, L.; Pokhrel, S. Safe-by-design CuO nanoparticles via Fe-doping, Cu-O bond length variation, and biological assessment in cells and zebrafish embryos. *ACS Nano*, **2017**, *11*, 501-515.

43. Hajipour, P.; Bahrami, A.; Eslami, A.; Hosseini-Abari, A.; Ranjbar, H. H. Chemical bath synthesis of CuO-GO-Ag nanocomposites with enhanced antibacterial properties. *J Alloys Comp.*, **2020**, *821*, 153456-1-7.

44. Kumar, S. R. K.; Mamatha, G. P.; Muralidhara, H. B.; Anantha, M. S.; Yallappa, S.; Hungund, B. S.; Kumar, K. Y. Highly efficient multipurpose graphene oxide embedded with copper oxide nanohybrid for electrochemical sensors and biomedical applications. *J Sci. Adv. Mater. Devices*, **2017**, *2*, 493-500.

45. Radziuk, D.; Mikhnavets, L.; Vorokhta, M.; Matolín, V.; Tabulina, L.; Labunov, V. Sonochemical formation of copper/iron-modified graphene oxide nanocomposites for ketorolac delivery. *Chem. Eur. J*, **2019**, *25*, 6233-6245.

46. Suslick, K. S. Sonochemistry. *Science*, **1990**, *247*, 1439-1445.

47. Suslick, K. S.; Eddingsaas, N. C.; Flannigan, D. J.; Hopkins, S. D.; Xu, H. The chemical history of a bubble. *Acc. Chem. Res*., **2018**, *51*, 2169-2178.

48. Nagvenkar, A. P.; Perelshtein, I.; Piunno, Y.; Mantecca, P.; Gedanken, A. Sonochemical one-step synthesis of polymer-capped metal oxide nanocolloids: antibacterial activity and cytotoxicity. *ACS Omega*, **2019**, *4*, 13631-13639.

49. Maruthapandi, M.; Nagvenkar, A. P.; Perelshtein, I.; Gedanken, A. Carbon-dot initiated synthesis of polypyrrole and polypyrrole@CuO micro/nanoparticles with enhanced antibacterial activity. *ACS Appl. Polym. Mater.*, **2019**, *15*, 1181-1186.

50. Beasley, D. E.; Koltz, A. M.; Lambert, J. E.; Fierer, N.; Dunn, R. R. The evolution of stomach acidity and its relevance to the human microbiome. *PLOS One*, **2015**, *10*, e0134116.

51. Fallingborg, J. Intraluminal pH of the human gastrointestinal tract. *Dan. Med. Bull.*, **1999**, *46*, 183-196.

52. Quigley, E. M.; Turnberg, L. A. pH of the microclimate lining human gastric and duodenal mucosa in vivo. Studies in control subjects and in duodenal ulcer patients. *Gastroenterology*, **1987**, *92*, 1876-1884.

53. Marcano, D. C.; Kosynkin, D. V.; Berlin, J. M.; Sinitskii, A.; Sun, Z.; Slesarev, A.; Alemany, L. B.; Lu, W.; Tour, J. M. Improved synthesis of graphene oxide. *ACS Nano*, **2010**, *4*, 4806-4814.

54. Radziuk, D.; Mikhnavets, L.; Tkach, A.; Tabulina, L.; Labunov, V. Sonochemically assembled photoluminescent copper-modified graphene oxide microspheres. *Langmuir*, **2018**, *34*, 8599-8610.

55. Edwards, L. J. The dissolution and diffusion of aspirin in aqueous media. *Trans. Faraday Soc.*, **1951**, *47*, 1191-1210.

56. Fini, A.; Fazio, G.; Feroci, G. Solubility and solubilization properties of non-steroidal anti-inflammatory drugs. *Int. J. Pharm.*, **1995**, *126*, 95-102.

57. Margulis, M. A.; Margulis, I. M. Calorimetric method for measurement of acoustic power absorbed in a volume of a liquid. *Ultrason. Sonochem*., **2003**, *10*, 343-345.

58. Bhattacharjee, S. DLS and zeta potential - What they are and what they are not? *J. Control. Release*, **2016**, *235*, 337-351.

59. Krishnamoorthy, K.; Veerapandian, M.; Yun, K.; Kim, S.-J. The chemical and structural analysis of graphene oxide with different degrees of oxidation. *Carbon*, **2013**, *53*, 38-49.

60. El-Trass, A.; ElShamy, H.; El-Mehasseb, I.; El-Kemary, M. CuO nanoparticles: synthesis, characterization, optical properties and interaction with amino acids. *Appl. Surf. Sci*., **2012**, *258*, 2997-3001.

61. Li, D.; Muller, M. B.; Gilje, S.; Kaner, R. B.; Wallace, G. G. Processable aqueous dispersions of graphene nanosheets. N*at. Nanotechnol*., **2008**, *3*, 101-105.

62. Pegau, W. S.; Zaneveld, J. R. V. Temperature dependent absorption of water in the red and near infrared portions of the spectrum. *Limnol. Oceanogr.*, **1993**, *38*, 188-192.

63. Jia, W.; Reitz, E.; Sun, H.; Li, B.; Zhang, H.; Lei, Y. From $Cu_2(OH)_3Cl$ to nanostructured sisal-like $Cu(OH)_2$ and CuO: synthesis and characterization. *J. Appl. Phys*., **2009**, *105*, 064917-1-6.

64. Xu, H.; Suslick, K. S. Sonochemical preparation of functionalized graphenes. *J. Am. Chem. Soc.*, **2011**, *133*, 9148-9151.

65. Kumar, R. V.; Diamant, Y.; Gedanken, A. Sonochemical synthesis and characterization of nanometer-size transition metal oxides from metal acetates. *Chem. Mater.*, **2000**, *12*, 2301-2305.

66. Luche, J.-L. A few questions on the sonochemistry of solutions. *Ultrason. Sonochem.*, **1997**, *4*, 211-215.

67. a) Debbichi, L.; Marco de Lucas, M. C.; Pierson, J. F.; Krüger, P. Vibrational properties of CuO and Cu_4O_3 from first-principles calculations, and Raman and Infrared spectroscopy. *J. Phys. Chem. C,* **2012**, *116*, 10232-10237; b) Speier, G., Tyeklár, Z. Formation of carboxylate copper oxygen complexes in the reaction of metallic copper

with 1,2-dicarbonyls and dioxygen. *Transition Met. Chem.*, **1992**, *17*, 348-351; c) Nyquist, R. A.; Kagel, R. O. Infrared spectra of inorganic compounds; Academic Press: New York and London, **1971**; p 220; d) Kliche, G.; Popovic, Z. V. Far-infrared spectroscopic investigations on CuO. *Phys. Rev. B*, **1990**, *42*, 10060-10066.

68. a) Rainsford, K. D. (Ed.); Aspirin and Related Drugs; CRC Press, Boca Raton, USA, **2004,** pp. 800; b) Iwunze, M. O. Absorptiometric determination of acetylsalicylic acid in aqueous ethanolic solution. *J Anal. Lett.*, **2008**, *41*, 2944-2953; c) Kitamura, K.; Majima, R. Determination of salicylic acid in aspirin powder by second derivative ultraviolet spectrometry. *J Anal. Chem*., **1983**, *55*, 54-56.

69. a) Palomo, M. E.; Ballesteros, M. P.; Frutos, P. Analysis of diclofenac sodium and derivatives. *J Pharm. Biomed. Anal*., **1999**, *21*, 83-94; b) M.Cid-Cerón, M.; Guzmán-Hernández, D. S.; Ramírez-Silva, M. T.; Galano, A.; Romero-Romo, M.; Palomar-Pardavé, M. New insights on the kinetics and mechanism of the electrochemical oxidation of diclofenac in neutral aqueous medium. *Electrochim. Acta*, **2016**, *199*, 92-98; c) Matin, A. A.; Farajzadeh, M. A.; Jouyban, A. A simple spectrophotometric method for determination of sodium diclofenac in pharmaceutical formulations. *Farmaco*, **2005**, *60*, 855-858.

70. Chen, X. Y.; Cui, H.; Liu, P.; Yang, G. W. Shape-induced ultraviolet absorption of CuO shuttlelike nanoparticles. *Appl. Phys. Lett*., **2007**, *90*, 183118.

Table of Contents Graphic

Ultrasound (20 kHz) causes complexation of pristine acetylsalicylic acid and diclofenac with preformed graphene oxide-CuO nanoparticles via specific binding involving Cu-O and C-H bonds, and H-bond formation with the carboxylic and carbonyl groups of the drug and GO.